

Desaturation and structure relationships around drifts excavated in the well-compacted Tournemire's argillite (Aveyron, France)

Jean Michel Matray*, Sébastien Savoye, Justo Cabrera

IRSN, DEI/SARG-BP17–92262 Fontenay-Aux-Roses, France

Received 27 April 2006; received in revised form 18 September 2006; accepted 29 September 2006

Available online 24 January 2007

Abstract

This study aimed to explore the relationships between the extension of rock desaturation and the Excavation Damaged Zone (EDZ) subsequent to the excavation of a century-old tunnel and of recent drifts (1996 and 2003) at the Tournemire Underground Research Laboratory (URL) located in the Aveyron county (South of the *Massif Central*, France). The other objective of this work was to assess the impact of desaturation on the hydraulic head profile measured around the tunnel. One section was selected per drift. Two boreholes were drilled for each section: one parallel and one inclined (45°) with respect to the bedding. For each borehole, we performed on-site drill core mapping, petrophysical measurements, pneumatic and hydraulic tests by means of a Modular Mini-Packer System (MMPS). Results indicate that the EDZ around drifts is mainly a combination of unloading joints, mimicking the drift shape, and of desaturation cracks, parallel to the bedding. The EDZ extension around the tunnel is twice to three times that of the drifts of 1996 and 2003 and is essentially composed of unloading joints resulting from the mechanical response of the rock. The masonry covering the tunnel walls is assumed to have protected the rock from seasonal variations of air humidity, thus limiting (without excluding) the formation of desaturation cracks. The EDZ extension deduced from core mapping is in agreement with that deduced from pneumatic tests with permeabilities several orders of magnitude greater than in the undisturbed zone. Degrees of saturation for the three sections range between 0.9 and 1 in the EDZ area and reach 1 in the undamaged zone. The head profile deduced from measurements recorded since 2002 indicates the occurrence of an Excavation Disturbed Zone (EdZ) of about 40 m around the tunnel. This EdZ is likely due to the existence of sub-atmospheric water pressures clearly seen in the first meter around the tunnel. We have tried to quantify the impact of the tunnel since its excavation on saturation degree and on hydraulic heads. The simulation was performed by considering, as a first approach, the absence of fracturing in the EDZ. A constant suction of -3300 m, deduced from the mean annual values of relative humidity and temperature measured in the tunnel atmosphere since 2002, was applied at the tunnel wall. The degrees of saturation simulated around the tunnel are underestimated in the EDZ area and consistent to experimental data in the unfractured zone. The modelling of hydraulic heads is overestimated in the horizontal direction and is in the domain of experimental values in the vertical direction, but the lack of intermediate data cannot enable us to conclude on this consistency. This study demonstrated the role played by fracturing on the distribution of petrophysical parameters and of heads around drifts and the century-old tunnel. It has also demonstrated the necessity of coupling mechanic and hydraulic calculations by considering capillary forces.

© 2006 Elsevier B.V. All rights reserved.

Keywords: Tournemire; Argillite; Permeability; EDZ; EdZ; Desaturation

* Corresponding author. Tel.: +33 1 58 99 05.

E-mail address: jean-michel.matray@irsn.fr (J.-M. Matray).

1. Introduction

Argillaceous formations are considered in several European countries as potential repository host rocks for high-level radioactive wastes in deep geological formations. Their very low water velocity (due to a very low permeability and diffusivity and a moderately low hydraulic gradient) coupled to a large thickness (several hundreds of meters) and a high sorption capacity make these rocks potentially interesting for a repository as radionuclide transfer times should exceed several times the radionuclide half-lives. However, the construction of a repository can lead to perturbations due to excavation works and the subsequent decompression of the surrounding rocks, ventilation of the underground drifts or construction of the engineered barriers. Host rock properties around underground openings (tunnels, drifts and niches) are likely altered during and after excavation works. Plastic deformations are especially expected in an altered zone called excavation damaged zone (EDZ), depending on the mechanical properties, the initial stress field and excavation techniques (Bossart et al., 2002). A fracture network consisting of unloading fractures and desaturation cracks is developed in this EDZ with hydraulic conductivities orders of magnitude higher than those of the unaltered zone. This fracture network can thus facilitate the transfer of radionuclides towards the biosphere along galleries and shafts in case of radionuclide release from waste containers and tightness failure of engineered barriers. It can also modify the petrophysical properties of the claystone around the openings. Porosity and water content are amongst the most sensitive properties due to relaxing of the constraints and to hydration/dehydration cycles under low humidity conditions (Charpentier et al., 2003). Ventilation of the underground drifts and shafts during the construction and the operation phases can induce the partial desaturation of the rock around the drift, thus modifying its thermo-hydromechanical properties (Mayor et al., 2005). This change in rock properties affects a zone around excavations called Excavation disturbed Zone (EdZ) which may have an impact on the design of the potential repository (drift spacing and repository size). One of the greatest perturbations concerns the distribution of the hydraulic profiles around excavations.

To evaluate the impact of excavations, and more particularly, of desaturation on the hydraulic and petrophysical properties of a claystone, the French Institute of Radioprotection and Nuclear Safety (IRSN) has been conducting research programmes since 1991 in its underground research laboratory of Tournemire, in the Aveyron county (south of France). The Tournemire URL

crosses a Toarcian argillaceous formation *via* a century-old tunnel and its adjacent drifts excavated in 1996 and in 2003. The tunnel and drifts are naturally ventilated since their excavation with a mean annual relative humidity and temperature of $74.7\% \pm 14.7$ and $11.2\text{ }^\circ\text{C} \pm 1.7$ respectively and for a record period of 4 years. This natural ventilation is likely responsible for the partial desaturation of the rock (Ramambasoa, 2001; Valès et al., 2004).

This paper aims to characterize the extent of desaturation around the century-old tunnel and drifts of the URL and to understand the role of this desaturation on the petrophysical and hydraulic properties of the rock.

Characterization has been performed by means of 6 cored boreholes, with 2 boreholes per openings (century-old tunnel, drift 1996 and drift 2003), one parallel to the bedding and the second with a dip angle of 45° down at the intersection of the drift and the ground to access the area assumed to be most fractured of the EDZ but also for assessing the time and tunnel-shape dependency on desaturation.

For each drift and tunnel, in these boreholes discontinuities (unloading and tectonic joints), petrophysical properties (total porosity, gravimetric water content, degree of saturation and volumetric moisture content) have been analyzed. In parallel, permeability, hydraulic conductivities and transmissivities have been determined in each borehole by means of pneumatic and hydraulic tests.

The role of desaturation on the petrophysical and hydraulic properties of the rock around galleries is then assessed by comparing the hydraulic heads estimated around the tunnel after *in situ* pressure measurements to hydraulic heads obtained from a numerical simulation performed since the tunnel excavation. This preliminary modelling was performed without taking into account the mechanical aspects, by means of VS2DT 3.0, a computer program developed by the U.S. Geological Survey for solving problems of water flow and solute transport in variably saturated porous media (Lappala et al., 1983; Hsieh et al., 1999).

2. Geological, structural, mechanical and hydrogeological background

The Tournemire URL is located in a Mesozoic marine basin on the southern border of the French *Massif Central* and at the western limit of the *Causse du Larzac*. The studied argillaceous formation is 250 m-thick and corresponds to sub-horizontal consolidated argillaceous and marly layer of Toarcian and Domerian age (Fig. 1). This formation is sandwiched between two carbonated and karstified aquifers (Cabrerá et al., 2001; Patriarche et al., 2004).

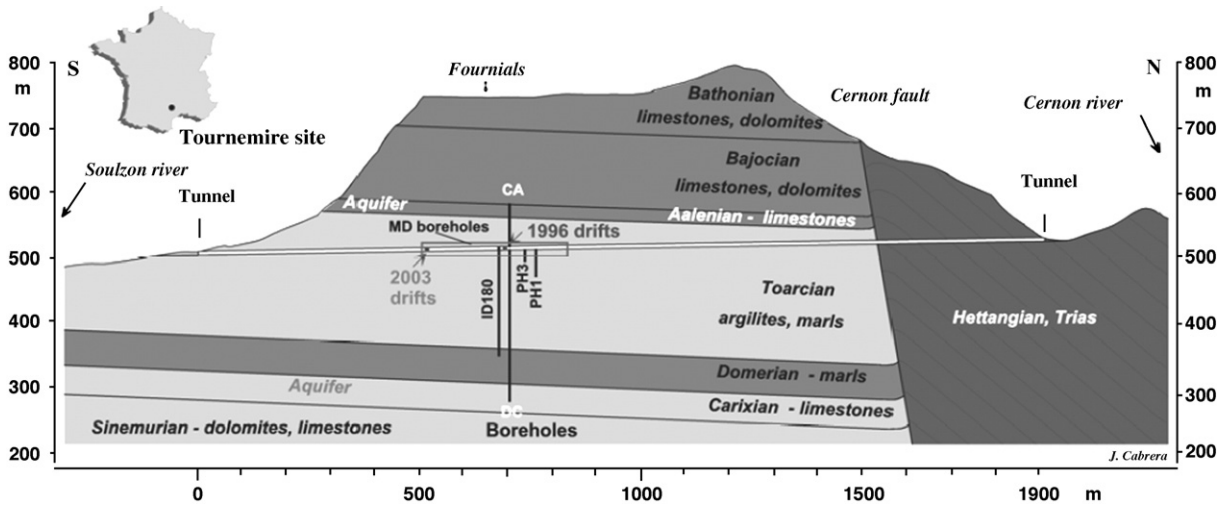


Fig. 1. Geological cross section of the Tournemire URL.

The Tournemire massif is a monocline structure with a mean dip angle of about -4° to the North. The lower (Hettangian to Carixian series) and upper (Aalenian to Bathonian series) aquifers are 300 m and 250 m thick respectively and essentially composed of limestone and dolomite. The argillaceous formation is composed of 250 m of well-compacted and thinly bedded claystones

and marls. [Peyaud et al. \(2005\)](#) suggested on the basis of results obtained from fission tracks analyses, that the argillaceous formation was buried over 1300 ± 400 m of sediments more than those observed at present, thus explaining the present state of over-consolidation of the clayey formation. The clay fraction ranges between 20 and 50% of the bulk rock. It is mainly composed of illite

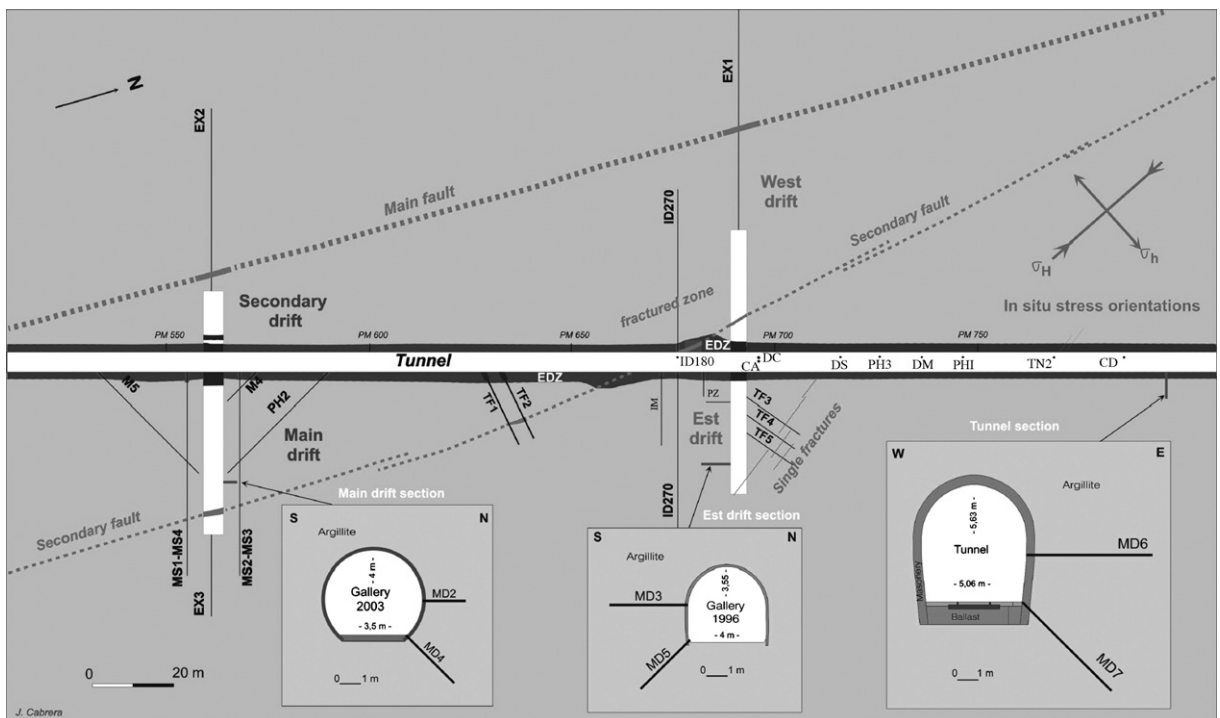


Fig. 2. Boreholes location and sections in the structural context of the Tournemire URL.

(5 to 15%), illite/smectite mixed-layer minerals (5 to 10% with a smectitic proportion of about 10%), chlorite (1 to 5%) and kaolinite (15–20%). The claystone also contains 10 to 20% of quartz grains, 10 to 40% of carbonates (mainly composed of calcite with traces of dolomite and siderite) and 2 to 7% of pyrite (Cabrera et al., 2001; Savoye et al., 2001, 2006). The upper Toarcian is crossed by an 1885 m long and century-old railway tunnel excavated between 1882 and 1886. This tunnel was an excellent opportunity for IRSN (formerly IPSN) to have an easy access to an argillaceous formation and develop its own research programmes and for training its experts in evaluating the possibilities and processes of radionuclide transport in this kind of rock.

The Tournemire massif is separated by a reverse and very transmissive major structure namely the Cernon fault (80 km long, Fig. 1). This regional fault has a kilometric extension roughly oriented West–East that enables the communication between the two surrounding aquifers. The argillaceous formation is also affected by a main fault and secondary subvertical faults of hectometric extension and oriented N170–180°E (Fig. 2), *i.e.* close to the maximal horizontal stress direction $\sigma_H = N162 \pm 15^\circ E$ for

a minimal horizontal stress $\sigma_h = N72 \pm 15^\circ E$. Both directions were determined through hydraulic fracturing tests conducted on boreholes (Rejeb and Tijani, 2003). The results suggest the occurrence of an anisotropic stress field with $\sigma_v = 3.8$ MPa, $\sigma_h = 2.1$ MPa and $\sigma_H = 4.0$ MPa (Rejeb and Cabrera, 2006). Because most faults date from the Pyrenean compression during the Eocene (from 53 to 33 Ma), and because the Cernon fault preceded them, the argillites likely acquired their rigidity and subsequent susceptibility to fracturing under mechanical stress quite early in the massif history (Patriarche et al., 2004).

The secondary fractures are generally partially sealed with calcite and give access to unfractured blocks of argillite characterized by hydraulic conductivities amongst the smallest reported in the world (between 10^{-14} and 10^{-15} m/s *i.e.* 10^{-21} and 10^{-22} m² as intrinsic permeabilities) for a specific storativity of *ca* 10^{-6} m⁻¹ (Boisson et al., 1998; Cabrera et al., 2001; Fatmi et al., 2005). These secondary faults sometimes present geodic cavities located at the junctions of two faults that enable the vertical transfer of fluids. With the Cernon fault, these fractures are the only opportunity of getting fluids in contact with the clay formation. Hydraulic tests

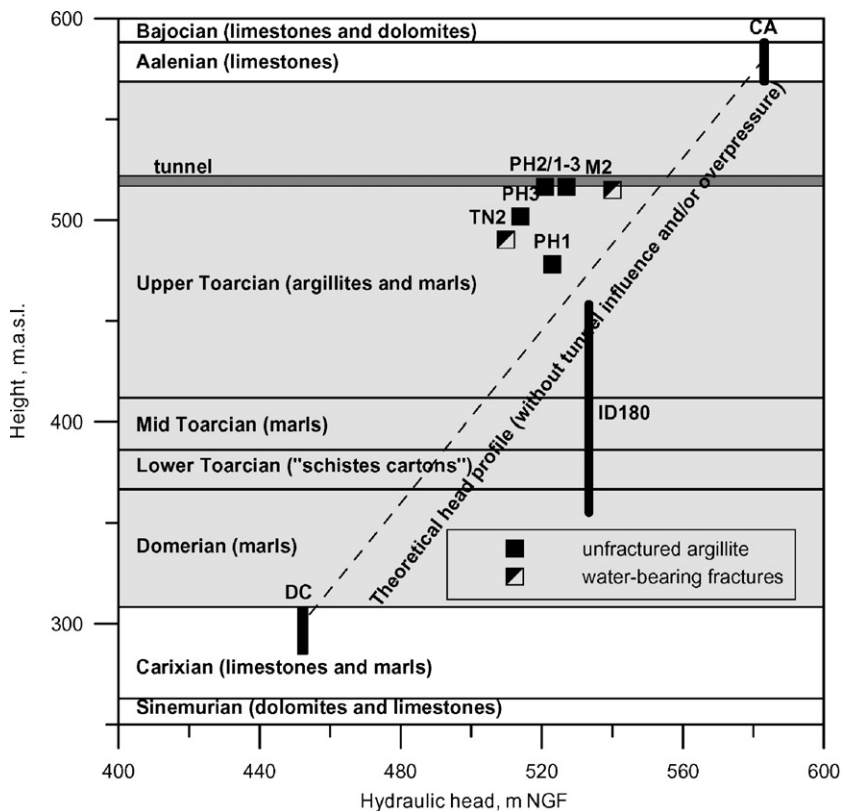


Fig. 3. Hydraulic head profile through the argillaceous formation at Tournemire.

Table 1
Extent of damaged zones around each underground openings (after Rejeb and Cabrera, 2006)

Openings	1881 tunnel	1996 gallery	2003 gallery
Fractures	Onion skins	Parallel to stratification	Parallel to stratification
EDZ	0.22 R	0.20 R	0.16 R

performed on these fault junctions have supplied relatively high transmissivities (around 10^{-10} m²/s) *i.e.* with permeabilities orders of magnitude higher than those of the unfractured zone and for an equivalent tested height (Savoye et al., 2003). Fig. 3 shows the distribution of the stabilized hydraulic heads with respect to boreholes CA and DC located in the tunnel axis. Pressures have been measured in the unfractured zone with permanent sealed probes (boreholes PH1 and PH3) and a multipacker system (borehole PH2). Hydraulic heads were also measured in the water-bearing fractures by means of double packer devices (boreholes TN2, M2 and ID180, see Fig. 2). Fig. 3 shows a depression of *ca* 30–40 m around the tunnel with respect to the theoretical hydraulic head profile drawn from heads measured in the two aquifers ($H_{CA}=583$ m NGF and $H_{DC}=453$ m NGF). This theoretical profile excludes any tunnel influence or a possible overpressure. This region is characterized by the occurrence of sub-atmospheric water pressures limited to the first meter around the tunnel (see desaturation results in Section 4) and constitutes a capillary fringe (Horseman et al., 1996) as a consequence of tunnel excavation and natural ventilation. In contrast, the hydraulic head measured in an 80 m height test section in the lower part of the argillaceous formation and isolating a water-bearing fracture likely indicates the occurrence of an overpressure in the argillite.

Two other fracture networks exist at the Tournemire URL that may have an important role on water flow and transport of dissolved species. These networks are

essentially confined around the tunnel and drifts. The first one is due to the stress redistribution during excavation and subsequent rock convergence. This mechanical behavior is governed by the anisotropic character of the argillite. Values of the elastic modulus, Poisson's coefficients, shear modulus and uniaxial compressive strengths are $E_1=27,680$ MPa, $\nu_1=0.17$, $E_2=9270$ MPa, $\nu_2=0.20$ and $G_{12}=3940$ MPa, $\sigma_{C1}=32$ MPa and $\sigma_{C2}=13$ MPa, respectively with 1 and 2 referring to parallel and normal to the bedding (Rejeb and Cabrera, 2006). The size of the EDZ around each opening is reported in Table 1 (after Rejeb and Cabrera, 2006). The second network is made of subhorizontal fractures at the drift wall and developed parallel to the bedding (several meters deep each with a millimetric aperture and a frequency of about 1 per 10 cm). This network is directly linked to seasonal variations of the drifts' atmosphere (hygrometry and temperature) and attributed to variations in the chemical potential of the interstitial solutions under swelling/shrinking cycles (Ramambasoa, 2001; Valès et al., 2004). Indeed, the drift hygrometry recorded since 1999 indicates seasonal variations (40% RH and 8 °C in winter and 100% and 14 °C in summer) with a mean annual RH value of 77% leading to a partial evaporation of the interstitial water. There is a clear correlation between this network aperture and hygrometry with a lag time of about 60 h between the fracture aperture recorded by means of extensometers and RH variations measured with capacitive thermo-hygrometers (Fatmi et al., 2004).

3. Materials and methods

3.1. Borehole drilling

Six single core boreholes with lengths ranging between 1 and 6 m were air-drilled between June 2004 and February 2005 from the tunnel and the experimental drifts excavated in 1996 and 2003. Boreholes were drilled

Table 2
Main objectives (C for petrophysical measurements, H hydraulic tests, P pneumatic tests) and characteristics of boreholes drilled in the framework of this study

ID/ section	Aim	Date	Drift (distance from the tunnel)	Azimuth	Dip angle	Length	Height of borehole head/ground
					Degree		
MD2/A	C/H/P	29/06/04	Drift 2003 (27 m N wall)	N15	0° sub-parallel to bedding	2.07	1.6
MD3/B	C/H/P	12/10/04	Drift 1996 (23 m)	N195	0° sub-parallel to bedding	3.58	1.5
MD4/A	C/P	22/11/04	Drift 2003 (27 m)	N15	45° down	3.41	1.6
MD5/B	C/P	23/11/04	Drift 1996 (23 m)	N15	45° down	3.22	1.5
MD6/C	C/H/P	23/02/05	Tunnel 1885	N105	0° sub-parallel to bedding	6.00	1.87
MD7/C	C/P	22/02/05	Tunnel 1885	N105	45° down	6.00	1.87

Section A, B and C refers respectively to gallery 2003, gallery 1996 and century-old tunnel.

with a Hilti device and supplied core samples of about 35 cm long each with a diameter of 55 mm. Borehole locations are shown in Fig. 2 and their main characteristics summarized in Table 2.

3.2. Drill core mapping

The core analysis and photo documentation were performed immediately after their removal from boreholes and just before the plug preparation for petrophysical measurements. A thorough structural analysis reported on core tried to distinguish between fracturing related to the excavation works and the subsequent desaturation on the one hand, and that induced by tectonic events.

3.3. Petrophysical measurements by water content and volume determinations

Immediately after the visual description, the cores were sawed on-site in plugs 34 cm long each. The following parameters were determined: total porosity, volumetric moisture content, gravimetric water content and degree of saturation as a function of the distance from the borehole mouth. The total mass of the humid samples (M_{tot}) was measured right after sawing. Then, the total apparent volume of the humid samples (V_{tot}) was determined following the method detailed in Monnier et al. (1973) that uses Archimedes' principle by weighing the displacement of petroleum (kerdane: a de-aromatised oil) with a Sartorius YDK 01 density measurement kit. This determination has required (i) to saturate sample in petroleum just after the M_{tot} measurement, (ii) the determination of the relationship between the kerdane density and temperature (iii) plus additional measurements among which the mass of humid sample in the air after saturation in oil (W_a) and the sample mass after immersion in petroleum (W_p). The

plugs were then oven dried at 105 °C and 150 °C until stabilization (*i.e.* after 2 to 4 days for each temperature) for measuring their respective masses M_{105° , M_{150° . All masses were determined on-site with the same accurate scale (OHAUS, type Adventurer AR3130 having a repeatability of 0.001 g for masses ranging between 0 and 310 g). The grain density (ρ_s) was obtained by He-pycnometry with a mean value of 2.704 g cm⁻³ at 105 °C and 2.703 g cm⁻³ at 150 °C for a standard deviation of 0.004 g cm⁻³. The water density (ρ_w) was calculated from an estimation of the interstitial water to 1.0012 g cm⁻³ with a standard deviation of 0.0004 g cm⁻³. The definitions of functions are those reported in Annex 10 in Pearson et al. (2003). The total or physical porosity (n_{tot} , dimensionless) is the ratio of the pore volume to total apparent volume ($n_{tot} = V_{pores} / V_{tot}$ with $V_{pores} = V_{tot} - V_{solids} = V_{tot} - M_{105^\circ/150^\circ} / \rho_{s105^\circ/150^\circ}$ where $\rho_{s105^\circ/150^\circ}$ is the grain density obtained at 105 °C or 150 °C). The gravimetric water content, dry mass basis ($WC_{dry, 105 \text{ or } 150^\circ}$, dimensionless) is the ratio of the mass of water ($M_w = M_{tot} - M_{105^\circ}$ where M_{tot} represents the total mass of the humid sample) and the oven-dry mass M_{105° or M_{150° such as $WC_{dry, 105 \text{ or } 150^\circ} = 100 \times (M_w / M_{105 \text{ or } 150^\circ})$. The degree of saturation (S , dimensionless) is the ratio of water-filled to total pore space ($S = V_w / V_{pores}$ with $V_w = (M_{tot} - M_{105^\circ/150^\circ}) / \rho_w$). The volumetric moisture content (θ , dimensionless) is the ratio of water-filled pore space to total volume (V_w / V_{tot}) and becomes a function of the degree of saturation (S) and of total porosity such as: $\theta = S_r \times n_{tot}$.

In addition, some SEM observations performed at IRSN verified the occurrence or absence of heavy minerals like pyrite and lighter minerals like carbonates, which have an important impact on the grain density of samples.

Errors on functions $U = F(V_1, V_2, \dots)$ were estimated by propagation of the analytical errors variances following the classical Gauss formula ($\sigma_U^2 = \sigma_{V_1}^2 (\partial F / \partial V_1)^2 + \sigma_{V_2}^2 (\partial F / \partial V_2)^2 + \dots$ in Theoria combinationis, 1821).

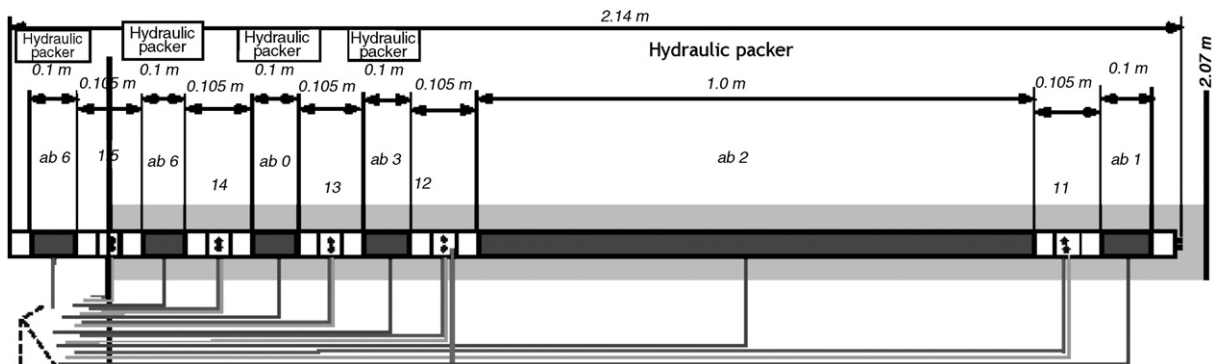


Fig. 4. Schematic view of the MMPS device.

3.4. Pneumatic and hydraulic tests

The MMPS (Modular Mini-Packer System) equipment was initially designed for hydraulic testing in the excavation disturbed zone of the Mont Terri Laboratory (Cottour et al., 1999). It allows up to five individual packer modules with a diameter of 52 mm to be coupled in a variety of configurations. Each packer module consists in a stand-alone unit with a packer inflation line and both flow and pressure measurement lines. Packer pressures are controlled by a manometer installed at the control unit, while both a manometer and a pressure transducer control interval pressures. The configuration of the MMPS is shown in the Fig. 4. A series of four 10.5-cm intervals separated through four 10-cm packers were applied. Further away, a 100-cm packer and a last 10-cm packer located at the bottom of the MMPS were installed such that a fifth 10.5-cm interval (Fig. 4) allows a less disturbed zone to be simultaneously characterized. The use of 1-m length extension tubes permits the investigation of an area up to 5 m (in the tunnel boreholes). Pneumatic tests were performed prior to hydraulic testing to provide an estimate of both the extent and the connectivity of the fracture network and also semi-quantitative estimates of interval permeability of the tested intervals.

3.4.1. Pneumatic testing

Pneumatic tests have already been performed in consolidated argillaceous rocks in the Mont Terri's URL with the aim of characterizing the EDZ extension (Bossart et al., 2002). They inject nitrogen or pump air in/out of the interval; the corresponding pneumatic response with the MMPS device is then interpreted. The surface test equipment allows working with injection and extraction flow rates between 0.1 and 50 l/min at standard conditions.

The MMPS was set into the boreholes immediately after their completion. Packers were inflated to 20 to 25 bars to limit the possibility of packer bypass. Afterwards, during the injection of nitrogen or the extraction of air using a vacuum pump, the air flow rates and the pressures in the test and observation intervals were recorded with a data acquisition system. A test was stopped when steady-state conditions were either reached or the pressure and flow rate measurements indicated a permeability below the detection limit of about $5 \times 10^{-17} \text{ m}^2$. The detection limit was reached when flow rates dropped below the measurement limit during air extraction tests or when pressures during injection tests were completely dominated by wellbore storage effects. The estimate of gas permeability was

deduced from a steady-state approximation of pneumatic test data as described in detail by Bossart et al. (2002).

3.4.2. Hydraulic testing

Three types of hydraulic tests were performed: (i) injection tests at constant head performed right after initial pressure recovery in intervals crossing water-bearing fractures; (ii) pulse tests carried out in intervals showing a value of gas permeability under the detection limit ($5 \times 10^{-17} \text{ m}^2$), thus indicating that rock should be water-saturated, *i.e.* without occurrence of connected fractures. This kind of test was performed right after pneumatic testing, thus inducing an overestimation of transmissivity as the initial pressure was not achieved; (iii) injection tests at constant head in intervals crossing very transmissive single fractures as in the EDZ to verify estimates from pneumatic tests. All test intervals were saturated with a synthetic water, the composition of which was as close as possible to that of interstitial waters to avoid any osmotic and chemical effects. This water (Table 3) was made similar to the average composition of fracture waters collected in the argillite at the tunnel level (Beaucaire et al., submitted for publication). In the third case, single fractures were firstly artificially saturated by circulating this synthetic water for one day.

The pulse test data were analyzed using the method developed by Bredehoeft and Papadopoulos (1980) and the constant head injection test using a straight line analysis (Jacob and Lohman, 1952) on a pressure vs log time plot (see Bossart et al., 2002 for details). The following relationship was used to compare the transmissivity estimates from hydraulic testing with the permeability estimates from pneumatic testing:

$$k = \frac{T\mu}{h\rho g}$$

Where k : permeability (m^2); T : transmissivity estimate from hydraulic testing ($\text{m}^2 \text{ s}^{-1}$); μ : viscosity of water ($1.002 \times 10^{-3} \text{ Pa s}$ at $20 \text{ }^\circ\text{C}$); h : test interval length

Table 3

Chemical composition of the synthetic water used for saturating tests intervals during hydraulic tests

Anions (mmol L ⁻¹)		Cations (mmol L ⁻¹)	
Cl ⁻	6.5	Na ⁺	9.5
HCO ₃ ⁻	4	K ⁺	0.22
		Ca ²⁺	0.085
		Mg ²⁺	0.38

It represents the average composition of waters collected in boreholes crossing water-producing fractures at the tunnel level (TF5 and M2, location reported in Fig. 1) after Beaucaire et al. (submitted for publication).

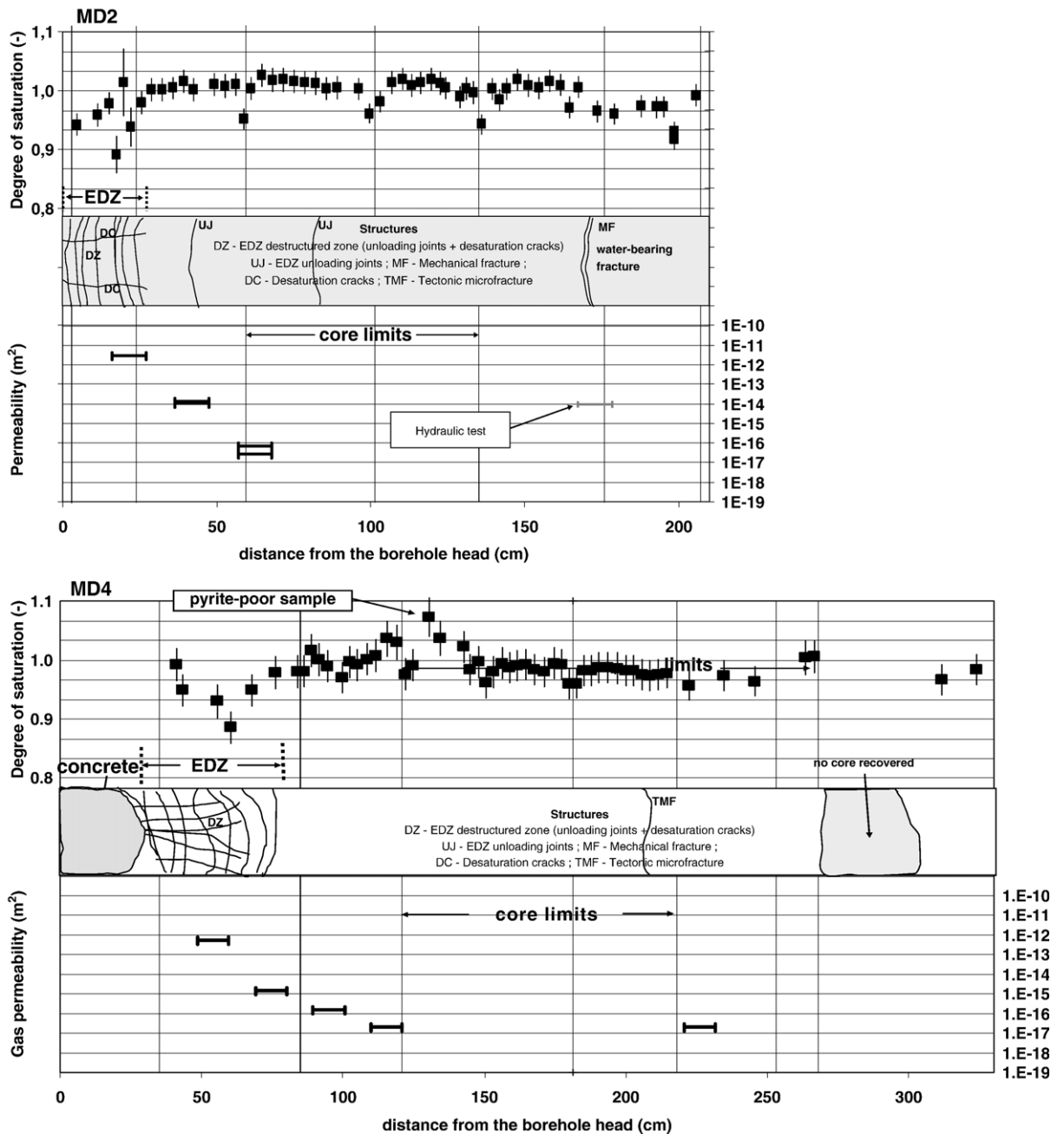


Fig. 5. Drill core mapping, gas permeability and degree of saturation as a function of distance for boreholes MD2 and MD4 drilled from the drift 2003.

(usually $h=0.105$ m); ρ : density of water (1000 kg/m³); g : gravity acceleration (9.81 m s⁻²).

4. Results

All data are shown for each section in Figs. 5–7 as a function of the distance from the borehole head. Each figure reports results obtained on the two boreholes of a

same section (A for drift 2003, B for drift 1996 and C for the century-old tunnel). For each borehole, are given the drill core mapping showing the extension of the EDZ, the degree of saturation calculated from petrophysical measurements of sample volumes and masses for samples oven dried at 105 °C, permeability determined from pneumatic test and permeability recalculated from transmissivity values obtained from hydraulic tests. The

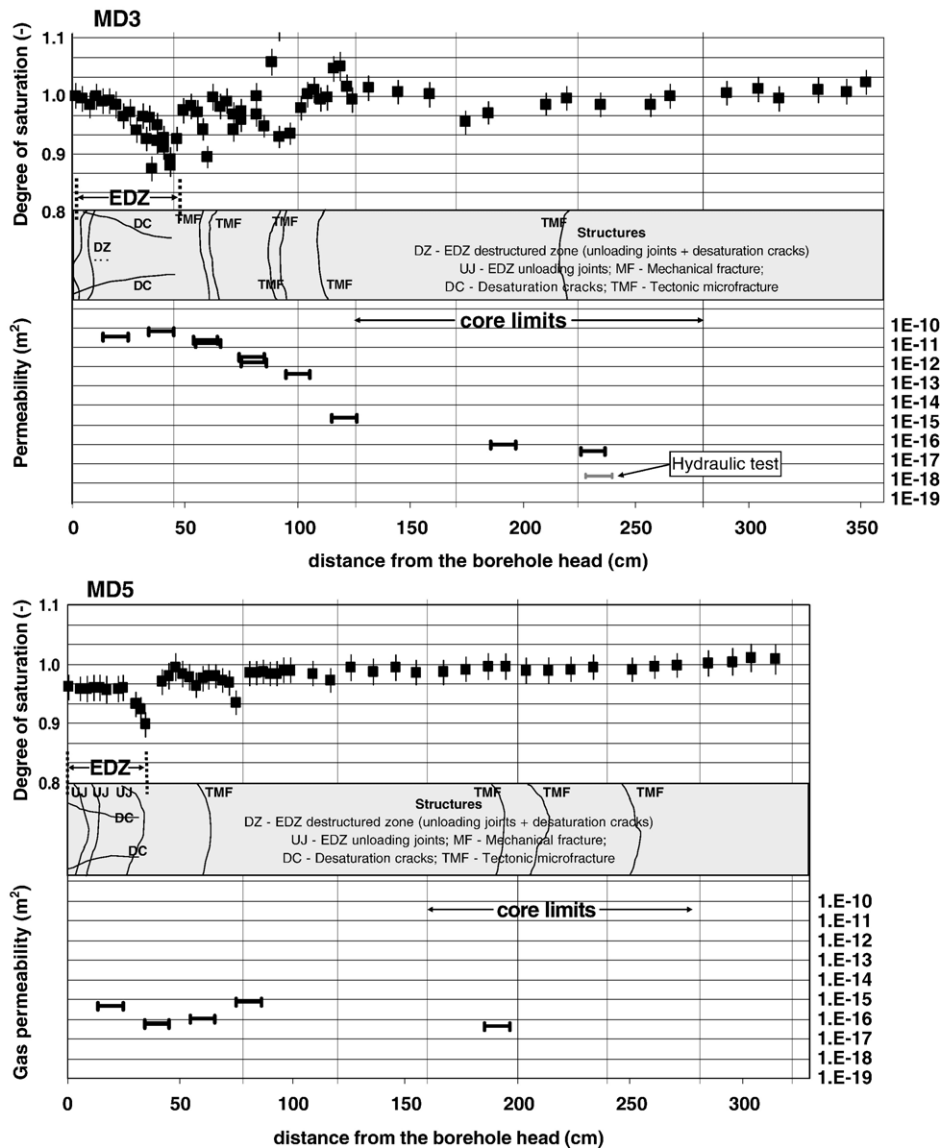


Fig. 6. Drill core mapping, gas permeability and degree of saturation as a function of distance for boreholes MD3 and MD5 drilled from the drift 1996.

average petrophysical properties determined inside and outside the EDZ areas are summarized in Table 4. Due to the similar results obtained in the first borehole at 105 and 150 °C (Table 4), we decided to only oven-dry at 105 °C.

4.1. Section A (drift 2003)

The drill core mapping shows a destructured (DZ) Excavation Disturbed Zone (EDZ) with an extension of about 30 cm and 50 cm in MD2 (horizontal) and MD4 (inclined), respectively. Those damaged zones are

characterized by a High Density Fracturation (HDF) combining unloading joints (UJ) (mimicking the gallery shape) and desaturation cracks (DC), parallel to the bedding. Borehole MD2 also shows the occurrence of isolated unloading joints at distances of about 40 and 70 cm and of a water-bearing mechanical fracture (MF). MF is a fracture assumed to be induced by the stress redistribution during the gallery excavation. This fracture has likely captured water from fractures of tectonic origin as suggested by their chemical and isotopic compositions close to those collected on water-bearing tectonic fractures (Beaucaire et al., submitted for publication). In

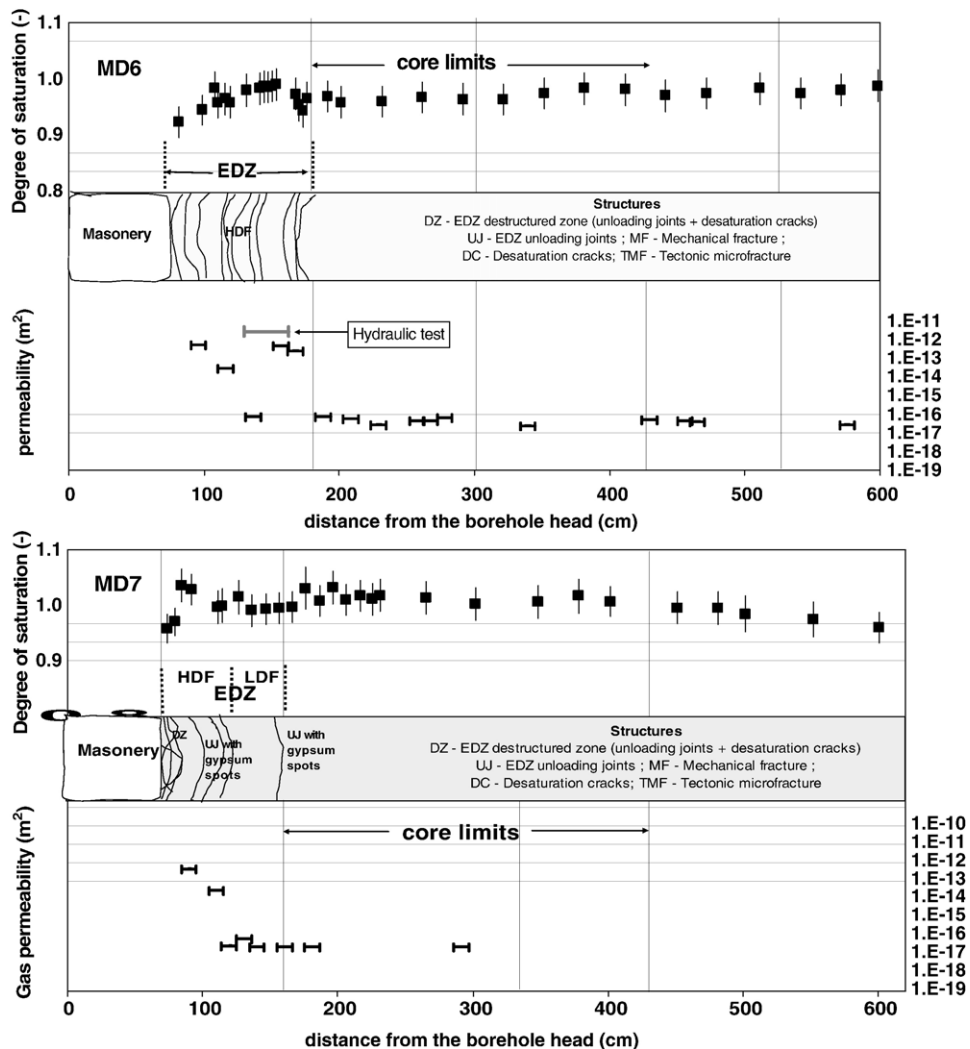


Fig. 7. Drill core mapping, gas permeability and degree of saturation as a function of distance for boreholes MD6 and MD7 drilled from the century-old tunnel.

further support of this hypothesis, the very low matrix permeability cannot explain the production of such amount of water since the beginning of the gallery excavation (about 1 year). One calcite-filled microfracture of tectonic origin is also observed in MD4.

Table 4 shows that petrophysical parameters inside the EDZ are systematically lower than the outside, except for MD4 where the very first centimeters are saturated. We assume that water used for the concrete floor of the gallery has partially re-saturated the clayey matrix before its hardening. Except for this area, both boreholes show a desaturation trend in the damaged zones with values increasing from 95% in MD4 and 98% in MD2 at the borehole mouth up to about 100% close to the EDZ outer border with an error of *ca* 3%.

Outside the EDZ, the rock may be considered as fully saturated. There are also two other artefacts. The first one is artificial and refers to strong desaturation trends at the core limits as a consequence of an overheating during the *in situ* core break and removal. The second type is natural and attributed to the presence or absence of heavy minerals like pyrite (density of 5 g cm^{-3}). Degrees of saturation greater than one as shown in MD4 are attributed to the second type after SEM observations.

The permeability profiles obtained from pneumatic tests show a progressive decrease of values from very high ($\geq 10^{-12} \text{ m}^2$) in the EDZ to very low values ($\leq 10^{-17} \text{ m}^2$) in the undisturbed zones. The extent of the partially-saturated zone is greater for MD2 than for MD4 and is explained by the presence of unloading joints up to about

Table 4

Average values of water content, total porosity, volumetric moisture content and degree of saturation determined inside and outside the EDZ areas at 105 °C

Borehole	EDZ	WC_{dry} , %	n_{tot} , %	θ , %	S , %
MD2	In	3.073±0.003	7.79±0.18	7.612±0.38	97.7±2.7
MD2	Out	4.085±0.003	9.92±0.18	9.93±0.37	100.1±1.8
MD2*	In	3.173±0.003	8.12±0.18	7.85±0.38	96.3±3.7
MD2*	Out	4.183±0.003	10.22±0.28	10.17±0.66	99.6±2.6
MD3	In	3.284±0.007	8.53±0.27	8.14±0.64	95.1±2.1
MD3	Out	3.562±0.005	8.87±0.18	8.77±0.65	98.9±2.5
MD4	In	3.891±0.021	9.95±0.28	9.51±0.64	95.2±2.7
MD4	Out	4.150±0.005	10.07±0.27	10.06±0.63	100.1±2.7
MD5	In	3.180±0.004	8.31±0.18	7.91±0.38	94.9±2.1
MD5	Out	3.456±0.004	8.67±0.18	8.53±0.37	98.6±2.1
MD6	In	3.670±0.003	9.29±0.27	9.04±0.64	96.9±2.8
MD6	Out	3.704±0.003	9.38±0.27	9.11±0.65	97.0±2.8
MD7	In	3.910±0.003	9.60±0.27	9.57±0.64	99.7±2.8
MD7	Out	3.783±0.004	9.26±0.27	9.29±0.64	100.3±2.9

*Data obtained at 150 °C.

70 cm from the borehole border in MD2. Hydraulic tests performed in the water-bearing fracture crossed in MD2 indicate a transmissivity of $ca\ 8.9 \times 10^{-9}\ m^2\ s^{-1}$.

4.2. Section B (drift 1996)

There is a bigger EDZ extension in MD3 (horizontal) than in MD5 (inclined). This result is due by a bigger extension of desaturation cracks reaching $ca\ 45\ cm$ and $30\ cm$ in MD3 and MD5, respectively. On the contrary, the EDZ unloading joints are limited to the very first $20\ cm$ in MD3 with a high density fracturation and reach up to $35\ cm$ in MD5 with a low density fracturation. Both boreholes also show the occurrence of tectonic microfractures filled with calcite.

As in Section A, the mean values of petrophysical parameters (Table 4) are systematically lower inside the EDZ than outside. There is no clear desaturation trend in MD3 but values as low as 94% are calculated up to about $80\ cm$. On the contrary, borehole MD5 shows a clear desaturation profile limited to the EDZ extent. In both boreholes border artefacts are observed as in Section A. The permeability profile obtained from pneumatic tests performed in MD3 shows a progressive decrease of values from $\geq 10^{-11}\ m^2$ in the very first $60\ cm$ down to $\leq 10^{-17}\ m^2$ at about $2\ m$, *i.e.* far away from the EDZ extension. The presence of tectonic fractures filled with calcite could explain this behavior. Permeabilities obtained in MD5 are much more lower ($10^{-16}\ m^2 < k < 10^{-15}\ m$) than for MD3. This behavior is quite similar to that observed in the inclined borehole MD4 from Section A. A hydraulic test was performed in the saturated area at a distance of $2.3\ m$ from the borehole head, giving a

transmissivity of $1.1 \times 10^{-12}\ m^2\ s^{-1}$, for an equivalent permeability of $10^{-18}\ m^2$, *i.e.* at least two orders of magnitude greater than it should be in the undisturbed zone.

4.3. Section C (century-old tunnel)

The drill core mapping shows an EDZ of about $1\ m$ in both MD6 (horizontal) and MD7 (inclined). High density fracturation of unloading joints concerns the whole EDZ in MD6 and only the first $50\ cm$ in MD7. The EDZ unloading joints observed in MD7 also show the occurrence of gypsum spots.

Table 4 shows that the MD6 petrophysical parameters are systematically lower inside the EDZ than outside. MD7 shows the inverse situation but uncertainties calculated for this borehole are so important that the real behavior may be overwhelmed by measurement errors.

The permeability profiles obtained from pneumatic tests performed in MD6 and MD7 show very high permeabilities in the High Density Fracturation zones with values ranging between 10^{-13} and $10^{-12}\ m^2$. An attempt of artificial saturation of this zone has allowed the conduction of a hydraulic test giving a transmissivity value of about $10^{-6}\ m^2\ s^{-1}$. This value gave an estimate of equivalent permeability of about $10^{-11}\ m^2$, *i.e.* very close to those estimated from pneumatic tests, like those performed under similar conditions at the Mont Terri underground rock laboratory (Bossart et al., 2002). Permeabilities calculated outside of these areas are likely less than the detection limit of pneumatic tests ($5 \times 10^{-17}\ m^2$).

5. Discussion

5.1. EDZ and desaturation extensions

The study of the fracture network from the drill core mapping shows that the extension of the EDZ at the Tournemire URL is a combination of unloading joints and of desaturation cracks. This extension is bigger around the tunnel (*ca* 1 m in both boreholes MD6 and MD7) than around drift 1996 (up to 45 cm from the horizontal MD3 and 30 cm from the inclined MD5) which in turn shows a bigger extension than around drift 2003 (around 30 cm in the horizontal borehole MD2 and up to 40 cm in the inclined MD4). Desaturation cracks are not visible around the tunnel contrary to the drifts. The masonry made of limestone blocks (70–80 cm thick) and covering the tunnel wall since the end of the excavation is likely protecting the rock from the natural ventilation of the tunnel and could therefore explain the lack of desaturation cracks around the tunnel. The uncovered drifts show the occurrence of desaturation cracks with a bigger extension in horizontal boreholes (MD3 and MD2) than in the inclined one (MD4 and MD5) as a consequence of cracks developed along the subhorizontal bedding planes. The extension of unloading joints decreases with the age of the structure (tunnel, drifts) and is generally bigger in inclined boreholes compared to the horizontal ones. Therefore, a time-dependency on the EDZ unloading joints' extension is suggested (Rejeb and Cabrera, 2006).

The permeability profiles determined from pneumatic and hydraulic tests perfectly fit the EDZ extension. Permeabilities are highest (between 10^{-11} and 10^{-12} m²) in the High Density Fracturation and Destructured Zones of the EDZ. They decrease progressively in the Low Density fracturation area to reach values below the detection limit of 5×10^{-17} m² in the undisturbed zone of the EDZ.

There is also a strong correlation between the desaturated area determined from petrophysical determinations with the extension of the EDZ deduced from the coupled study of core mapping and permeability measurements. With the exception of borehole MD7, all petrophysical parameters determined inside the EDZ are systematically lower than the outside. The degree of saturation reflects the evolution of the water content and total porosity which are clearly linked to the extent of the EDZ. Therefore, the lower porosities and water content determined in the EDZ are likely a consequence of unloading and capillary coupled forces. The analysis of the curves that relate specific-volume and water content (%) relative to imposed suctions indicates that

for an equivalent capillary pressure deduced from the mean annual tunnel hygrometry (74%), we are still in an area where any loss of water is accompanied by an equivalent reduction of volume as suggested in Altinier (2006).

5.2. Modelling of saturation profiles and hydraulic heads around the tunnel

The main objective of this preliminary modelling is to assess the capability of Richards desaturation model to reproduce both desaturation and pressure head data measured around the tunnel. In the Richards model (de Marsily, 1986; Genty et al., 2002), both water submitted to gravity and suction forces are taken into account. The Richards equation is solved with a finite difference formulation implemented in VS2DTI 3.0 code (Lappala et al., 1983; Hsieh et al., 1999). The fracturation observed in the EDZ is not considered here. Model input data are porosity n_{tot} , suction curves giving the relationship between saturation S_w and suction ψ expressed as a function of the pressure head h , permeability K expressed as a product of the saturated permeability K_s and the relative permeability curve K_r function of the pressure head. The expressions of $S_e(h)$ and $K_r(h)$ given below, were formulated following the van Genuchten model (van Genuchten, 1980), as follows:

$$S_e = \frac{1}{\left(1 + |\alpha h|^\beta\right)^{1-\frac{1}{\beta}}}$$

$$k_r = \left\{1 - |\alpha h|^{(\beta-1)} \left(1 + |\alpha h|^\beta\right)^{\left(\frac{1}{\beta}-1\right)}\right\}^2$$

$$\times \sqrt{\left(1 + |\alpha h|^\beta\right)^{\left(\frac{1}{\beta}-1\right)}}$$

Where α and β are the parameters of the van Genuchten model and S_e , the effective saturation expressed in terms of volumetric moisture content θ and residual moisture content θ_r .

$$S_e = \frac{\theta - \theta_r}{n_{\text{tot}} - \theta_r}$$

Lab and *in situ* hydraulic tests have allowed an estimate of a mean value for hydraulic conductivity of about 10^{-14} m s⁻¹ (Boisson et al., 2001; Bertrand et al., 2002). Parameters for the van Genuchten suction curve were deduced from lab data obtained by Daupley (1997): $\alpha = 1.510^{-4}$ m⁻¹, $\beta = 2.5$ and ($r = 0.0056$). The mean

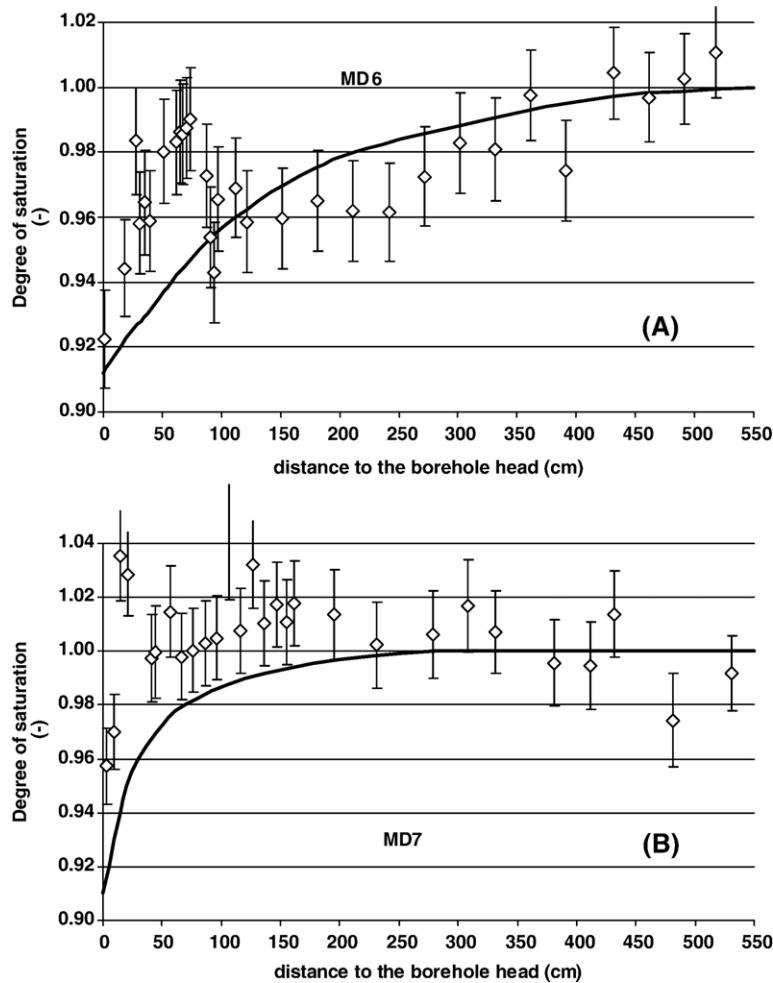


Fig. 8. Comparison of modeled degrees of saturation with measured ones (A) in borehole MD6 and (B) in borehole MD7.

value of total porosity measured in this study was equal to 9% (Table 4).

As the purpose of the calculations is to quantify the impact of the tunnel on the saturation degree and the hydraulic heads, the size of the simulated zone must also include domains outside the tunnel's influence. Thus, the 2D mesh consists of a $60\text{ m} \times 120\text{ m}$ rectangle in which a half tunnel is equidistant to the top, bottom and right side of the domain. The hydraulic boundary conditions were of the form: (i) hydrostatic conditions imposed by the two surrounding aquifers were applied at the upper and lower limits; (ii) a constant suction (-3300 m) was imposed at the tunnel wall. The capillary pressure value was derived from the temperature and relative humidity variations (Ramambasoa, 2001; Valès et al., 2004) measured in the tunnel using the Kelvin equation; (iii) a no-flow-boundary was applied at the others limits. The initial time for simulation is the year 1888, corresponding to the end of the tunnel excavation.

Fig. 8(A)–(B) compares the degrees of saturation simulated along boreholes MD6 and MD7 to values calculated from petrophysical data. Modelling results are roughly consistent to experimental data except in the EDZ where they are slightly lower. This discrepancy suggests that our single porosity model is likely smoothing the heterogeneities induced by the occurrence of fractures. The comparison between the simulated and the measured hydraulic heads is given in Fig. 9(A)–(B). The modelling of hydraulic heads in the vertical direction is in the domain of those measured in PH1 and PH3, but it is difficult to conclude on the consistency of this result with the measured data, because of the lack of *in situ* measurements at intermediate level. In the horizontal direction, the discrepancy between the simulated and the *in situ* values, especially in the deepest level, suggests that the influence of the tunnel would be greater than that derived from modelling. The presence of a high density fracturing made of unloading joints resulting from the mechanical

response of the rock to the present field of constraints and/or to the re-use of weakness plane of an ancient tectonic event could explain the occurrence of a capillary fringe around the tunnel. This fracturing is assumed to have increased the penetration depth of the suction effect and explains that the measured hydraulic heads are less than the simulated one. The extension of this depression may reach several tens of meters around the tunnel and makes part of the Excavation hydraulic disturbed Zone (EdZ). More complex modelling involving hydromechanical coupled modelling codes have been performed for predicting the EDZ extension under saturated and unsaturated conditions. Results indicate that the high deviatoric stress can cause failure and development of radial fractures around the tunnel rather than the “onion skin” orthoradial fractures observed in the true situation (after Rejeb et al., 2006). The comparison of modelling performed in the framework of this paper to the hydro-mechanical coupled one will help to verify the role played by desaturation cracks on the hydraulic head profiles.

6. Conclusions

The purpose of this study was twofold. Firstly, to explore the relationships between rock desaturation subsequent to the excavation of a century-old tunnel and modern drifts (1996 and 2003) and the EDZ extension. Secondly, to assess the impact of this desaturation on the hydraulic head profile measured around the tunnel and the drifts. One section was selected per structure (drift 2003, drift 1996 and century-old tunnel). We drilled two new boreholes for each section: one parallel to the bedding and the other one inclined downward at 45° at the gallery wall and ground intersection. For each borehole, we performed on-site drill core mapping, petrophysical measurements and finally, pneumatic and hydraulic tests by means of a Modular Mini-Packer System (MMPS).

Results indicate that the EDZ around drifts is mainly a combination of unloading joints, mimicking the drift shape, and of desaturation cracks, parallel to the

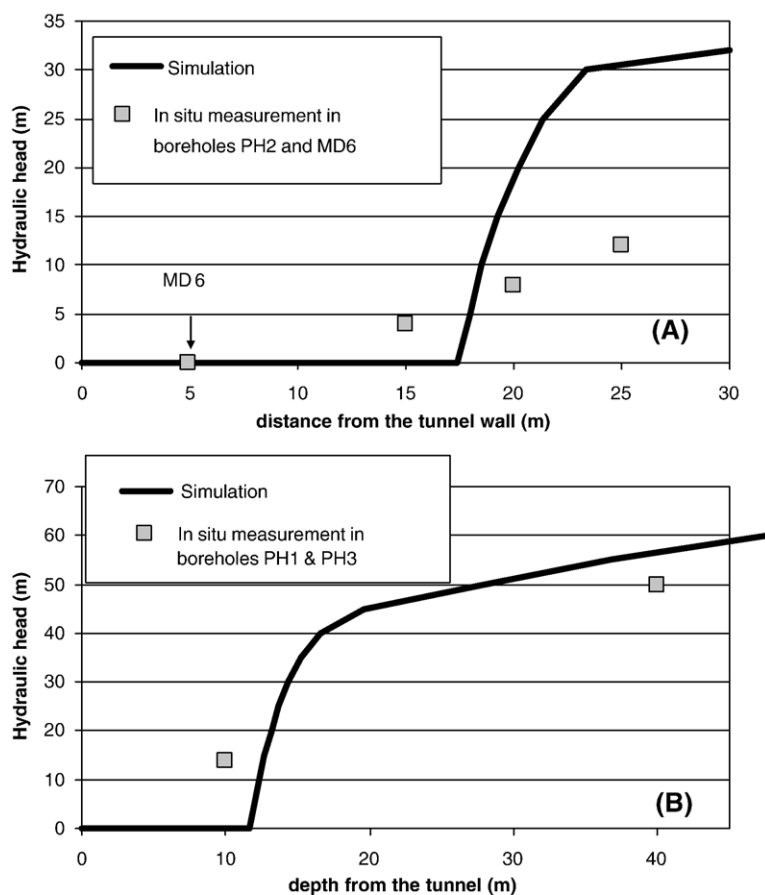


Fig. 9. Comparison of modeled hydraulic with measured ones (A) in horizontal direction and (B) in vertical direction. Only positive simulated hydraulic head values were represented in the figure for clarity reasons and all negative ones were fixed at zero.

bedding. The EDZ extension around the tunnel is twice to three times that of drifts 1996 and 2003 and essentially composed of unloading joints resulting from the mechanical response of the rock to the present field of constraints or to the resumption of an ancient tectonic damage. The masonry covering the tunnel walls is assumed to have protected the rock from the seasonal variations of the air humidity, thus limiting (without excluding) the formation of desaturation cracks. The EDZ extension deduced from core mapping is also in agreement with that deduced from pneumatic tests with permeabilities several orders of magnitude greater than in the undisturbed zone. Degrees of saturation deduced from petrophysical measurements for the three sections range between 0.9 and 1 in the EDZ area and reached saturation in the undamaged zone. Hydraulic heads are measured since 2002 by permanent pressure probes installed in the unfractured rock around the tunnel and by piezometers installed in the surrounding aquifers. The head profile indicates the occurrence of sub-atmospheric water pressures with an extension of *ca* 40 m around the tunnel. We have searched to quantify the impact of the tunnel since its excavation on the degrees of saturation and the hydraulic heads. The simulation was performed with the VS2DTI 3.0 code by using the Richards desaturation model and considering, as a first approach, the absence of fracturing in the EDZ area. A constant suction of -3300 m, deduced from the mean annual values of relative humidity and temperature measured in the tunnel atmosphere since 2002, was applied at the tunnel wall. The degrees of saturation simulated around the tunnel are underestimated in the EDZ area and consistent to experimental data in the unfractured zone. The modelling of hydraulic heads is overestimated in the horizontal direction and is in the domain of experimental values in the vertical direction, but the lack of intermediate data does not allow us to conclude on this consistency. The occurrence of an unloading joints fracture network resulting from the mechanical response of the rock to the present field of constraints or to the re-use of weakness zones of an ancient tectonic event is assumed to have created very high capillary pressures in the EDZ and could therefore explain discrepancies between the observed and simulated hydraulic heads.

This study has demonstrated the role played by fracturing on the distribution of petrophysical parameters and of heads around drifts and the century-old tunnel. It has also demonstrated the necessity of coupling mechanic and hydraulic calculations by considering capillary forces. Such calculations will be performed in the next step.

Acknowledgments

Two anonymous reviewers are warmly acknowledged for their fruitful comments on the manuscript. The authors also gratefully acknowledge S. Lemius for his help when carrying out petrophysical measurements and M. Piedevache and M. Kech from Solexperts for performing pneumatic and hydraulic testing. We also wish to give our acknowledgement to C. Combes for drilling boreholes. We would like to fully acknowledge K. Ben Slimane for its fruitful comments on the manuscript. Finally, we express thanks to N. Van Meir for having greatly improved the English.

References

- Altinier, A.M., 2006. Etude de la composition isotopique des eaux porales de l'argilite de Tournemire: Inter-comparaison des méthodes de mesure et relation avec les paramètres pétrophysiques. Thèse de Doctorat de l'Université Paris-Sud.
- Beaucaire, C., Michelot, J.-L., Savoye, S., Cabrera, J. Groundwater characterisation and modelling of water-rock equilibria in the Tournemire argillaceous formation (Aveyron, France). Applied Geochemistry.
- Bertrand, L., Lavignerie, R., Cabrera, J., Matray, J.-M., Savoye, S., 2002. Instrument for measuring pore pressure and permeability in low permeability rock. International Meeting "Clays in Natural and Engineered for Radioactive Waste Confinement", Organized by ANDRA in Reims, Conference Proceeding, pp. 321–322.
- Boisson, J.Y., Cabrera, J., Bertrand, L., Heitz, J.F., 1998. Mesures de très faibles perméabilités in situ et en laboratoires sur les argilites de Tournemire (Aveyron). Méthodologies comparées et effet d'échelle. Bull. Soc. Géol. Fr. 169, 595–604.
- Boisson, J.Y., Bertrand, L., Heitz, J.F., Moreau-Le Golvan, Y., 2001. In situ and laboratory investigations of fluid flow through an argillaceous formation at different scales of space and time, Tournemire tunnel, southern France. Hydrogeol. J. 9, 108–123.
- Bossart, P., Meier, P.M., Moeri, A., Trick, T., Mayor, J.C., 2002. Geological and hydraulic characterisation of the excavation disturbed zone in the Opalinus Clay of the Mont Terri Rock Laboratory. Eng. Geol. 66, 19–38.
- Bredehoeft, J.D., Papadopoulos, S.S., 1980. A method for determining the hydraulic properties of tight formations. Water Resour. Res. 16, 233–238.
- Cabrera, J., Beaucaire, C., Bruno, G., De Windt, L., Genty, A., Ramanbasoa, N., Rejeb, A., Savoye, S., Volant, P., 2001. Projet Tournemire — Synthèse des programmes de recherche 1995–1999, Rapport IPSN DPRES/SERGD 01–19, Paris France.
- Charpentier, D., Tessier, D., Cathelineau, M., 2003. Shale microstructure evolution due to tunnel excavation after 100 years and impact of tectonic paleofracturing. Case of Tournemire, France. Eng. Geol. 70, 55–69.
- Cottour, Ph., Bigarré, P., Camus, P., Bauer-Plaindoux, C., Blümling, P., 1999. Evaluation of in-situ stresses. Comparison of techniques. In: Thury, M., Bossart, P. (Eds.), Results of the Hydrogeological, Geochemical and Geotechnical Experiments, Performed in 1996 and 1997. Swiss National Geological and Hydrogeological Survey. Geological Report, vol. 23, pp. 160–170.

- Daupley, X., 1997. Etude du potentiel de l'eau interstitielle d'une roche argileuse et des relations entre ses propriétés hydriques et mécaniques. Thèse de l'Ecole Nationale Supérieure des Mines de Paris.
- de Marsily, G., 1986. Quantitative Hydrogeology. Academic Press Inc., London.
- Fatmi, H., Mangin, A., Matray, J.M., 2004. Traitement et exploitation des séries temporelles de pression, température et humidité obtenues sur le site de Tournemire. Rapport IRSN/DEI/SARG 04–24. Paris, France.
- Fatmi, H., Mangin, A., Matray, J.M., Savoye, S., 2005. Treatment and exploitation of time series of pressure and temperature obtained in the Tournemire URL. 2nd International Meeting, March 14–18, Tours, France in Tours, 14–18, Clays in Natural & Engineered Barriers for Radioactive Waste Confinement, Abstract Book, p. 561.
- Genty, A., Bassot, S., Bruno, G., Cabrera, J., Le Potier, C., 2002. Modelling of desaturation experiments on Tournemire argillite samples. In: Auriault et al. (Eds.), Poromechanics, vol. II, pp. 437–443.
- Horseman, S.T., Higgo, J.J.W., Alexander, J., Harrington, J.F., 1996. Water, gas and solute movement through argillaceous media. OECD/NEA CC-96/1:290.
- Hsieh, P.A., Wingle, W., Healy, R.W., 1999. A graphical software package for simulating fluid flow and solute or energy transport in variably saturated porous media. US Geological Survey Report — Water Resources Investigations, vol. 99–4130.
- Jacob, C.E., Lohman, S.W., 1952. Nonsteady flow to a well of constant drawdown in an extensive aquifer. Trans. AGU 33, 559–569.
- Lappala, E.G., Healy, R.W., Weeks, E.P., 1983. Documentation of computer program VS2D to solve the equations of fluid flow in variably saturated porous media. US Geological Survey Report — Water Resources Investigations, vol. 83–4099.
- Mayor, J.C., Garcia-Sineriz, J.L., Velasco, M., Gomez-Hernandez, J., Lloret, A., Matray, J.M., Coste, F., Giraud, A., Rothfuchs, T., Marshall, P., Fierz, T., Klubertanz, G., 2005. Ventilation experiment in Opalinus Clay for the disposal of radioactive waste in underground repositories. (Project funded by the European Community under the 'EURATOM' Programme 1998–2002 under contract No. FIKWCT-2001-00126). EC Final Tech. Publ. Rept. CEC Nuclear Science & Technology Series Luxembourg pp. 41.
- Monnier, G., Stengel, P., Fies, J.C., 1973. Une méthode de mesure de la densité apparente de petits agglomérats terreux. Application à l'analyse de système de porosité du sol. Ann. Agron. 24, 533–545.
- Patriarche, D., Michelot, J.-L., Ledoux, E., Savoye, S., 2004. Diffusion as the main process for mass transport in very low water content argillites: 1. Chloride as a natural tracer for mass transport. Diffusion coefficient and concentration measurements in interstitial water. Water Resour. Res. 40, W01516. doi:10.1029/2003WR002600.
- Pearson, F.J., Arcos, D., Bath, A., Boisson, J.Y., Fernandez, A.M., Gabler, H.E., Gaucher, E., Gautschi, A., Griffault, L., Hernan, P., Waber, H.N., 2003. Mont Terri project — Geochemistry of water in the Opalinus Clay formation at the Mont Terri Rock Laboratory. Rapport de l'OFEG, Série Géologie, vol. 5. Bern, 319 pp.
- Peyaud, J.-B., Barbarand, J., Carter, A., Pagel, M., 2005. Mid-Cretaceous uplift and erosion on the northern margin of the Ligurian Tethys deduced from thermal history reconstruction. Int. J. Earth Sci. 94, 462–474.
- Ramambasoa, N., 2001. Etude du comportement hydromécanique des argillites: application au site de Tournemire. Thèse de l'Ecole Polytechnique.
- Rejeb, A., Tijani, M., 2003. Stress field in the Tournemire argillaceous. In situ measurements and interpretation. Rev. Fr. Géotech. 103, 75–84.
- Rejeb, A., Cabrera, J., 2006. Time-dependent evolution of the excavation damaged zone in the argillaceous Tournemire site. Invited Lecture in the GeoProc International Conference on Coupled T-H-M-C Processes in Geosystems: Fundamentals, Modelings, Experiments and Applications, May 22–25 Nanjing, P.R. China.
- Rejeb, A., Millard, A., Rouhabi, A., Tijani, M., 2006. Modelling approaches of the excavation damaged zone (EDZ) around the old tunnel at the argillaceous Tournemire site. Proceedings in the GeoProc International Conference on Coupled T-H-M-C Processes in Geosystems: Fundamentals, Modelings, Experiments and Applications, May 22–25 Nanjing, P.R. China.
- Savoye, S., de Windt, L., Beaucaire, C., Bruno, G., Guitard, N., 2001. Are artificial tracers conservative in argillaceous media? The Tournemire claystone case. In: Cidu (Ed.), Water Rock Interaction Proceedings, vol. 10, pp. 1383–1386.
- Savoye, S., Cabrera, J., Matray, J.M., 2003. Different hydraulic properties of single fractures in argillaceous medium: the case of the IRSN Tournemire site (France). IAH Conference IAH "Groundwaters in Fractured Rocks", Prague (Tchéquie), sept 2003, Conference Proceeding, pp. 47–50.
- Savoye, S., Michelot, J.L., Wittebroodt, C., Altinier, M.V., 2006. Contribution of the diffusive exchange method to the characterization of pore-water in consolidated argillaceous rocks. J. Contam. Hydrol. 86, 87–104.
- Valès, F., Nguyen Minh, D., Gharbi, H., Rejeb, A., 2004. Experimental study of the influence of the degree of saturation on physical and mechanical properties in Tournemire shale (France). Appl. Clay Sci. 26, 197–207.
- van Genuchten, M.T., 1980. A closed-form equation for predicting the hydraulic conductivity of unsaturated soils. Soil Sci. Soc. Am. 44, 892–898.